GEOCHEMICAL MODELING OF GROUND WATER IN THE VICINITY OF THE

PANTEX PLANT, SOUTHERN HIGH PLAINS, TEXAS

Alan E. Fryar and William F. Mullican III

September 1995

CONTENTS

Figures

Tables

INTRODUCTION

The Ogallala (High Plains) aquifer is the largest aquifer in the United States (Zwingle, 1993). Beneath the Southern High Plains of Texas, pumpage for irrigation and, to a lesser extent, for municipal, industrial, and domestic uses since the 1930's has caused water levels in the aquifer to decline locally more than 30 m (Knowles and others, 1982; Dugan and others, 1994). These declines have motivated numerous physically based studies of rates and sources of recharge to the Ogallala aquifer, as reviewed by Mullican and others (1994). However, hydrochemical studies have been fewer. Hydrochemical studies can complement physically based studies by delineating sources of recharge and rates of subsurface water movement as well as by elucidating controls on water quality. In particular, studies of compositional evolution during recharge to and flow within the Ogallala aquifer, such as have been conducted for other regional aquifers in North America (for example, Hendry and Schwartz, 1990; Plummer and others, 1990; Murphy and others, 1992), have been limited.

In this report, we discuss the results of solute-speciation modeling involving data from wells sampled by the Bureau of Economic Geology (BEG) in the vicinity of the Pantex Plant (fig. 1). For a subset of these wells, solute data and data on the isotopic compositions of waters, soil gases, and sediments have been entered into a reaction-path (net mass-transfer) model. We use speciation and reaction-path modeling together to (1) corroborate inferred sources of recharge, (2) constrain estimates of travel times through the unsaturated zones above and below the perched aquifers, and (3) identify plausible reactions controlling the composition of ground water.

SATURATION INDEX CALCULATIONS

Using the geochemical model NETPATH (Plummer and others, 1994) for individual wells, we determined the speciation of various elements in solution and calculated solute activities (concentrations corrected for electrostatic attraction with other solutes) to obtain saturation indices
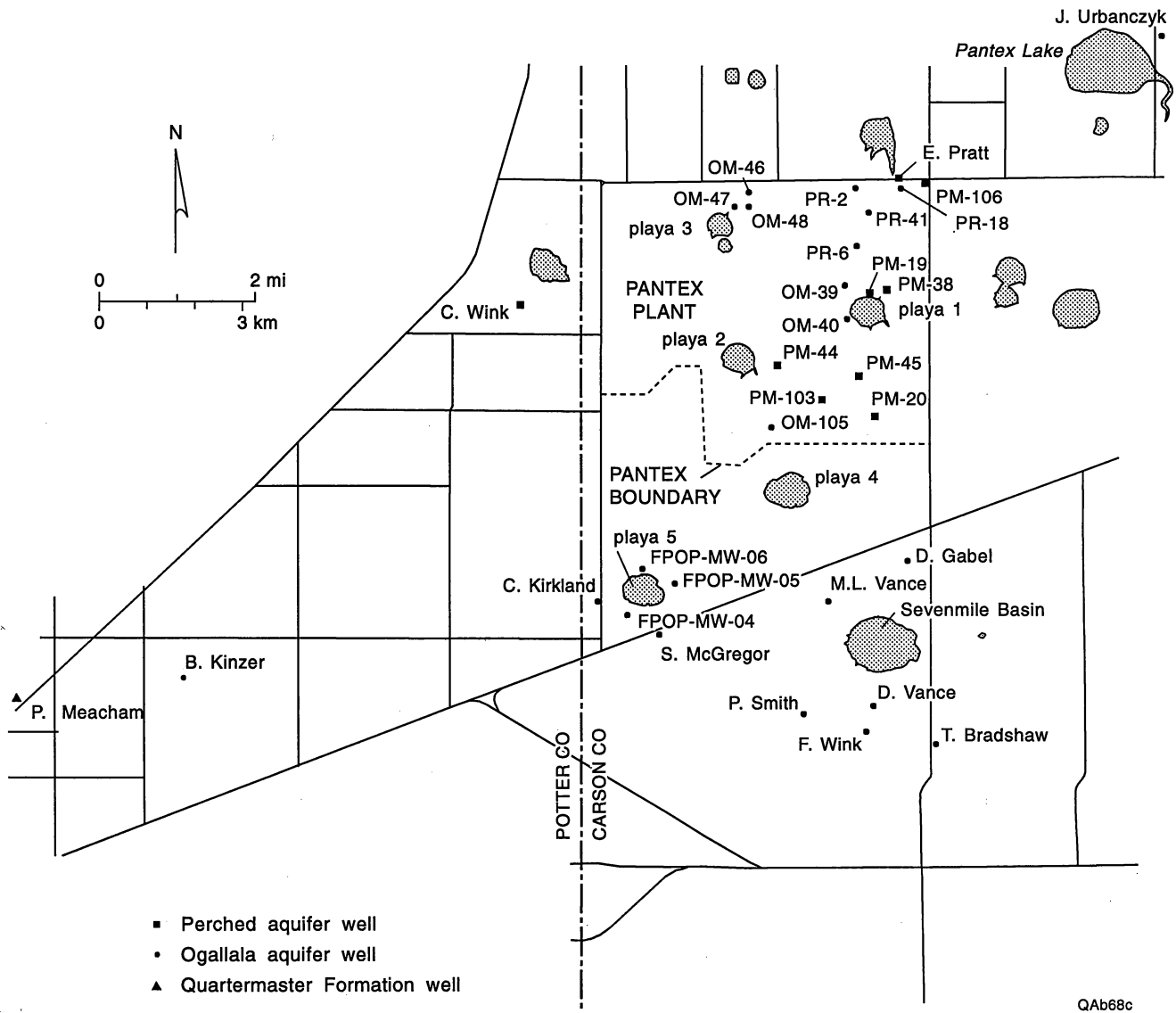
1

Figure 1. Location map of wells sampled by BEG in the area of the Pantex Plant. Landowners and/or tenants of private properties are indicated.

with respect to various minerals. The saturation index is defined as $SI = \log (IAP\ K_T^{-1})$, where IAP is the ion activity product for the ions comprising each mineral and K_T is the equilibrium solubility constant of the compound at the temperature of the solution. Supersaturation ($SI > 0$) indicates that precipitation of a compound is thermodynamically favorable, whereas undersaturation ($SI < 0$) indicates that dissolution is favored; saturation occurs at $SI = 0$. However, precipitation does not automatically accompany supersaturation; slow rates of reaction can inhibit precipitation.

Among major minerals, ground water ranges from nearly saturated to slightly supersaturated with respect to calcite (table 1). Even though quartz may be the predominant mineral on a volumetric basis within the Ogallala Formation, SiO_2 appears to neither precipitate nor dissolve within the perched and Ogallala aquifers. Ground water in the study area is supersaturated with respect to quartz and undersaturated with respect to amorphous silica (table 1). At temperatures characteristic of ground water (approximately 18°C), the rate of precipitation of quartz is sufficiently slow that direct precipitation of quartz is unlikely. Quartz would form via nucleation of amorphous silica if ground water were supersaturated with respect to amorphous silica (Steefel and van Cappellen, 1990). Because we are unaware of petrographic evidence for the presence of amorphous silica in the Ogallala Formation, we consider dissolution of that phase to be unlikely.

As suggested by thin-section and scanning electron microscopy (SEM) observations, dissolution of feldspars and precipitation of clay minerals may control the cycling of SiO_2 in the perched and Ogallala aquifers. Observations of vacuoles in feldspars provide plausible evidence of weathering (S. D. Hovorka, Bureau of Economic Geology, personal communication, 1995). SEM photomicrographs illustrate crystals of an unidentified authigenic clay mineral, possibly smectite, occasionally filling pores in core samples from the Ogallala aquifer, although the timing of such precipitation is unknown. Calculating saturation indices of feldspars and clay minerals (except for sepiolite, which is nonaluminous) is problematic because Al concentrations were uniformly below the detection limit of 0.24 to 0.27 mg L^{-1} by inductively coupled plasma-optical emission spectrometry. Al concentrations were above the inductively coupled plasma-mass spectrometry

Table 1. Saturation indices (SIs) for solid phases of interest for wells sampled by BEG.
SIs calculated using initial set of data for wells sampled on more than one occasion.

Well No.	SI calcite	SI am. silica	SI quartz	SI sepiolite
T. Bradshaw	-0.046	-0.34	0.979	-1.197
FPOP-MW-04	-0.087	-0.232	1.111	-1.125
FPOP-MW-05	-0.041	-0.378	0.927	-2.192
FPOP-MW-06	0.208	-0.369	0.954	-4.37
D. Gabel	0.052	-0.409	0.907	-0.965
B. Kinzer	0.045	-0.53	0.784	-1.49
C. Kirkland	0.591	-0.251	1.058	1.256
S. McGregor	0.062	-0.293	1.013	-0.884
P. Meacham	0.274	-0.316	1.004	0.262
OM-39	0.18	-0.502	0.802	-1.184
OM-40	0.029	-0.44	0.874	-1.588
OM-46	0.093	-0.499	0.814	-1.118
OM-47	0.043	-0.523	0.8	-1.786
OM-48	0.072	-0.53	0.793	-1.619
OM-105	0.05	-0.412	0.887	-1.525
PM-19	-0.051	-0.728	0.595	-5.828
PM-20	0.083	-0.585	0.736	-1.494
PM-38	0.061	-0.761	0.562	-5.008
PM-44	-0.002	-0.733	0.574	-2.604
PM-45	-0.018	-0.627	0.693	-2.772
PM-101	0.133	-0.62	0.695	-1.143
PM-103	0.427	-0.607	0.695	0.13
PM-106	1.529	-0.817	0.476	5.65
PR-2	0.283	-0.551	0.751	-1.034
PR-6	0.087	-0.491	0.821	-1.624
PR-18	-0.05	-0.536	0.764	-2.347
PR-41	0.067	-0.546	0.754	-1.946
E. Pratt	0.173	-0.669	0.637	-2.789
P. Smith	0.062	-0.353	0.976	-1.602
J. Urbanczyk	0.146	-0.49	0.82	-1.386
D. Vance	-0.025	-0.363	0.962	-1.609
M. L. Vance	-0.016	-0.276	1.045	-0.812
C. Wink	0.177	-0.706	0.569	-4.341
F. Wink	0.317	-0.34	0.965	-0.298

(ICP-MS) detection limit of 0.005 mg L^{-1} in 5 of 14 wells (OM-40, PM-44, PM-45, PR-2, and PR-6). NETPATH calculations using ICP-MS data for Al in those wells indicated undersaturation with respect to albite and anorthite and supersaturation with respect to K-feldspar, illite, Ca-smectite, and kaolinite (table 2). In 30 of 34 wells, ground water is undersaturated with respect to sepiolite (table 1).

To examine dissolution and precipitation of common aluminosilicates, we have constructed phase diagrams. We follow common practice (for example, Freeze and Cherry, 1979) in assuming that Al is conserved (maintained in the solid phase) in the weathering of aluminosilicates. Using NETPATH, we calculated the activity ratios of Na^+ to H^+ and of Ca^{2+} to $(H^+)^2$. By plotting the logarithm of each of these ratios versus the logarithm of the activity of $H_4SiO_4°$, we can determine whether water from a particular well lies in the stability field of (is prone to precipitate) a particular feldspar or clay mineral. Using the equilibrium thermodynamic relationships of Tardy (1971) for standard temperature and pressure (STP) (25°C and 1 atm), which reasonably approximate conditions in ground water, we observe that albite and anorthite are prone to dissolve and clay minerals are prone to precipitate (figs. 2 and 3). Tardy (1971) did not include sepiolite and palygorskite, which are globally uncommon but locally important in the Ogallala and Blackwater Draw Formations. (Palygorskite is also not included in the NETPATH thermodynamic data base.) Perched ground-water samples (except for PM-106, which is believed to be erroneous) plot close to the smectite–kaolinite boundary, suggesting equilibrium between those two phases, whereas Ogallala ground-water samples plot within the Na- and Ca-smectite stability fields. The absence of authigenic kaolinite, illite, and K-feldspar in SEM photomicrographs suggests that those phases are not currently precipitating from ground water in the study area. Appelo and Postma (1993, p. 214–215) noted that replacement of smectite by kaolinite may be impeded by slow reaction kinetics.

Apart from the assumption of STP conditions, other limitations to the use of phase diagrams should be noted. The kaolinite–gibbsite equilibrium constant given by Tardy (1971) has since been revised slightly (Robie and others, 1978); equilibrium constants for other reactions (and thus phase boundaries) may also have changed. More fundamentally, the thermodynamic relationships do not

Table 2. Saturation indices for aluminosilicate phases for wells in which Al concentrations measured by ICP-MS exceeded the detection limit of 5 μg/L (8.0 μg/L, OM-40; 8.8 μg/L, PM-44; 18.9 μg/L, PM-45; 32.5 μg/L, PR-2; 20.2 μg/L, PR-6).

	SI albite	SI anorthite	SI K-feldspar	SI illite	SI kaolinite	SI Ca-smectite
OM-40	-0.782	-2.85	1.05	2.68	4.05	3.28
PM-44	-1.91	-3.31	0.075	1.49	3.34	2.10
PM-45	-1.18	-2.34	0.927	3.27	4.92	3.99
PR-2	-0.47	-1.86	1.21	3.21	4.41	3.64
PR-6	-0.60	-2.11	1.24	3.31	4.63	3.91

account for variable compositions associated with solid-phase substitution. For example, the composition of smectite varies with substitution of Mg for Al in the octahedral sheets and substitution of Al for Si in the tetrahedral sheets of the crystal lattice. Na^+ and Ca^{2+} (and other monovalent and divalent cations) are electrostatically bound in the interlayers between tetrahedral sheets to satisfy charge deficiencies created by substitution.

REACTION-PATH MODELING

Phases and Constraints

Reaction paths have been modeled (1) between land surface and the perched aquifers; (2) along a hypothetical transect in the perched aquifers; and (3) between wells in the Ogallala aquifer, including mixing with water from the perched aquifers, to elucidate controls on the composition of ground water. Accounting for changes in solute chemistry along flowpaths allows us to estimate travel times on the basis of ^{14}C data and the proportions of recharge mixing with through-flowing ground water. We entered hydrochemical data for wells of interest into NETPATH (Plummer and others, 1994) and identified the solutes likely to constrain reactions in ground water and the possible phases (minerals, gases, organic matter, and ion exchange) involved (table 3). As a first approximation, end-member compositions were assumed for feldspars, clay

Figure 2. Activity-activity diagram depicting stability of Ca-smectite with respect to perched- (open-square) and Ogallala- (closed-circle) aquifer waters.

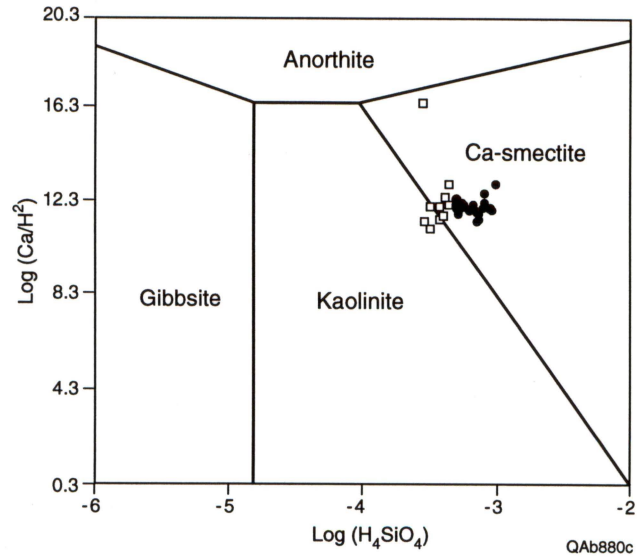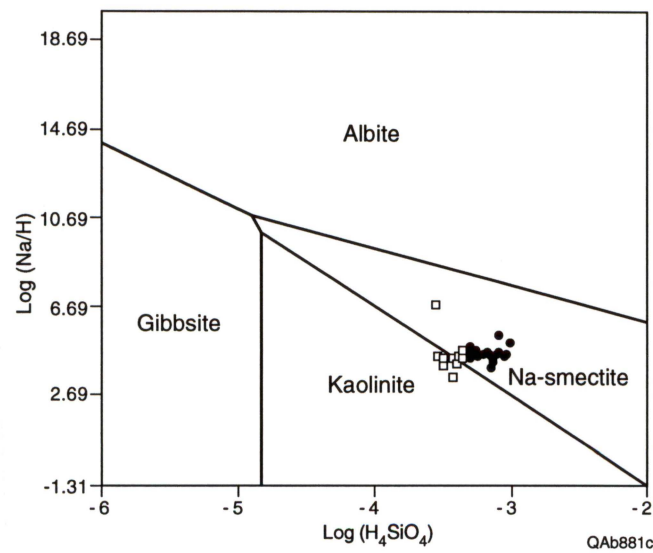

Figure 3. Activity-activity diagram depicting stability of Na-smectite with respect to perched- (open-square) and Ogallala- (closed-circle) aquifer waters.

Table 3. Constraints and phases used for NETPATH models.

Constraints	Phases
C	albite ($NaAlSi_3O_8$)
Ca	anorthite ($CaAl_2Si_2O_8$)
Al	calcite ($CaCO_3$)
Mg	Ca-smectite ($Ca_{0.125}Si_4(Al_{1.75}Mg_{0.25})(OH)_2O_{10}$)
Na	Na-smectite ($Na_{0.25}Si_4(Al_{1.75}Mg_{0.25})(OH)_2O_{10}$)
Si	palygorskite ($Mg_2Al_2Si_8O_{20}(OH)_2 \cdot 8H_2O$)
redox state†	sepiolite ($Mg_4Si_6O_{15}(OH)_2 \cdot 6H_2O$)
	CO_2 (g)
	O_2 (g)†
	CH_2O †
	Ca/Mg exchange
	Ca+Mg/Na exchange

† = land-surface–perched-aquifer models only

minerals, and calcite. The formulas for Na- and Ca-montmorillonite given by Tardy (1971) and

provided in the NETPATH data base actually refer to beidellite, the smectite end member

representing octahedral substitution. We modified the list of phases to include true

montmorillonite, the smectite end member representing tetrahedral substitution, which is much

more common than beidellite (Eslinger and Pevear, 1988; M. J. Dudas, Department of Soil

Science, University of Alberta, unpublished course notes, 1988).

We allowed ion exchange between Ca^{2+} and Mg^{2+} and between Na^+ and $Ca^{2+} + Mg^{2+}$

(ternary exchange, in which the ratio of Ca^{2+} to Mg^{2+} equaled the ratio in ground water in the final

well along a flowpath). Prior to reaction-path modeling, we calculated ranges in ion-activity

products (IAPs) for Na-Ca, Na-Mg, and Ca-Mg exchange for various wells according to the

equation

$$IAP = (N_B^{(1/z_B)}) \times (N_A^{(1/z_A)})^{-1} \times (a_A^{(1/z_A)}) \times (a_B^{(1/z_B)})^{-1} \times (K_N)^{-1}.$$

Here N is the equivalent adsorbed fraction (the ratio of the adsorbed cation concentration [in

meq 100 g^{-1}] to cation exchange capacity [CEC] or total exchangeable cations [TEC]), a is solute

activity, z is the valence, A and B represent the two cations in the exchange reaction, and K_N is the

8

selectivity coefficient (analogous to the equilibrium constant). Because measured CEC values were less than TEC values, we used TEC values to calculate IAPs. Ranges of IAP values, which were calculated because of variability in exchangeable cation concentrations, usually overlapped ranges of selectivity coefficients reported by Bruggenwert and Kamphorst (1982) and Appelo and Postma (1993, their table 5.5). Although approximating ternary exchange by two binary exchange reactions (Na-Ca and Na-Mg) is a simplification, the overlap between IAP values and selectivity coefficients suggests that exchange of major cations along flowpaths occurs reversibly.

The mass transfer module of NETPATH (NEWBAL) calculates the addition and loss of specified phases, accounting for mixing and evaporation where required, necessary to reproduce changes in solute chemistry between wells along a flowpath. The masses transferred for each combination of phases (defined as a reaction model) must honor the solute constraints specified by the user. However, the results are generally nonunique; multiple reaction models may be generated for a single flowpath. In addition, NEWBAL does not evaluate whether the reactions involved are thermodynamically feasible. Instead, the user is obligated to review the output from the speciation module to determine whether a given phase is subject to dissolution or precipitation.

NEWBAL also conducts isotopic mass-balance calculations, wherein dissolution of phases containing isotopes of interest (in our case, ^{13}C and ^{14}C) is nonfractionating and precipitation or exsolution of such phases follows a Rayleigh-distillation process with specified fractionation factors. Where C isotope data are involved, the isotopic mass balance is based on total dissolved C. Therefore, the isotopic composition of dissolved organic C (DOC) and of dissolving phases (for example, calcite and CO_2 gas) must be specified. Wells lacking data on DOC concentrations or on $\delta^{13}C$ of DOC were assigned values (some of which were averaged) from other wells in this study. For precipitation of calcite and exsolution of CO_2 gas, we selected the fractionation factors of Mook (1980). For each flowpath, the user must determine whether the difference between calculated and observed $\delta^{13}C$ values at the final well is acceptable (for example, within analytical uncertainty) and must recognize models in which ^{14}C-derived travel times are nonsensical (for example, <0 yr). We accepted reaction models for which (1) calculated $\delta^{13}C$ values were within

1‰ of observed values and (2) ^{14}C-derived travel times were within approximately an order of magnitude of independently derived values (based on ^{3}H data or velocity calculations using Darcy's law).

Land Surface to Perched Aquifers

Modeling chemical evolution between rainwater and perched ground water under natural recharge was limited by the small number of perched-aquifer wells unaffected by return flow. Based on the availability of isotopic data, we chose the C. Wink well and PM-44 to represent such wells adjacent to a playa and in an interplaya setting, respectively. For rainwater, we assumed $\delta^{13}C = -7‰$ (the average value for atmospheric CO_2 given by Keeling [1958]) and ^{14}C activity = 100 pmc. We used the precipitation-weighted average of major-ion concentrations (W. W. Wood, U.S. Geological Survey, and R. Nativ, Hebrew University of Jerusalem, unpublished data, 1993) and δD and $\delta^{18}O$ abundances (Nativ, 1988) measured on samples collected at Amarillo International Airport between October 1984 and September 1985. Because of evidence of OC oxidation beneath playas (Wood and Petraitis, 1984; Bennett and others, 1995), we initially included redox as a constraint and O_2 and CH_2O (representing OC) as phases. Ranges of $\delta^{13}C$ of playa-sediment OC (-15.4 to $-27.5‰$) and of vadose-zone CO_2 (-14 to $-27‰$) were taken from data provided by V. T. Holliday (Department of Geography, University of Wisconsin–Madison) and K. D. Romanak (Department of Geological Sciences, University of Texas at Austin), respectively. Following Keller (1991), we assumed that oxidation of OC does not fractionate ^{13}C, although Suchomel and others (1990) and Blair and others (1985) suggested that fractionation may be possible. We also assumed, as observed by Keller (1991), that ^{14}C of DOC = ^{14}C of DIC.

For simulations of playa-focused and interplaya recharge, we did not obtain plausible reaction models that included dissolution of O_2. Upon deleting O_2 as a phase, we obtained multiple plausible models that specified evaporation during playa-focused recharge (table 4). These models variously involved oxidation of OC; dissolution of CO_2 gas, anorthite, calcite, palygorskite, and

Table 4. Phases involved in plausible reaction models.

Rainwater— C. Wink (evaporation, redox)	Rainwater— C. Wink (no evaporation, redox)	Rainwater— C. Wink (evaporation, no redox)	Rainwater— C. Wink (no evaporation, no redox)	Rainwater— PM-44 (evaporation, redox)	Rainwater— PM-44 (evaporation, no redox)
anorthite +	albite +	anorthite +	albite +	albite +	calcite −
calcite +	anorthite +	calcite +	anorthite +	anorthite +	CO_2 (g) −
sepiolite ±	calcite +	sepiolite ±	calcite +	calcite ±	Ca+Mg/Na exch. +
palygorskite ±	sepiolite ±	palygorskite ±	sepiolite ±	sepiolite −	Mg/Ca exch. −
Ca-smectite −	palygorskite ±	Ca-smectite −	palygorskite ±	palygorskite −	
Na-smectite −	Ca-smectite −	Na-smectite −	Ca-smectite −	Ca-smectite −	
CH_2O +	Na-smectite −	CO_2 (g) +	Na-smectite −	Na-smectite −	
CO_2 (g) ±	CH_2O +	Ca+Mg/Na exch. −	CO_2 (g) +	CO_2 (g) −	
Ca+Mg/Na exch. −	CO_2 (g) +	Mg/Ca exch. ±	Ca+Mg/Na exch. ±	Ca+Mg/Na exch. ±	
Mg/Ca exch. ±	Ca+Mg/Na exch. ±		Mg/Ca exch. ±	Mg/Ca exch. −	
	Mg/Ca exch. ±				

OM-105+C. Wink+ PM-44 — OM-40	OM-105+C. Wink+ PM-44 — OM-39	OM-40+C. Wink— PR-41	OM-40+C. Wink+ PM-44 — PR-41
anorthite +	anorthite +	albite +	anorthite +
sepiolite +	sepiolite +	anorthite +	sepiolite +
Na-smectite −	palygorskite +	Ca-smectite −	palygorskite +
Mg/Ca exch. −	Ca-smectite −	CO_2 (g) −	Ca-smectite −
	Na-smectite −	Mg/Ca exch. −	Na-smectite −
	Mg/Ca exch. −		Ca+Mg/Na exch. +

1. For each transect, not all phases were necessarily involved in each model.
2. For minerals, CH20, and CO2 (g), + = precipitation, − = dissolution, and ± = precipitation or dissolution.
3. For Ca+Mg/Na exchange, + = Ca+Mg adsorption and Na desorption; − = Na adsorption and Ca+Mg desorption.
4. For Mg/Ca exchange, + = Mg adsorption and Ca desorption; − = Ca adsorption and Mg desorption.

sepiolite; precipitation of Ca- and Na-smectite, palygorskite, and sepiolite; exsolution of CO_2 gas; and ion exchange. For interplaya recharge with evaporation, plausible models involved oxidation of OC; dissolution of albite, anorthite, and calcite; precipitation of calcite, Ca- and Na-smectite, palygorskite, and sepiolite; exsolution of CO_2 gas; and ion exchange. Model-derived evaporation factors ranged from 8.09 to 49.2 for C. Wink and 8.51 to 103 for PM-44. Evaporation factors calculated independently using Cl^- (dividing concentrations in ground water by the weighted average concentration in precipitation) are 5.6 for C. Wink and ≤ 25 for PM-44. Cl^--based evaporation factors may overestimate actual evaporation during episodic recharge. Therefore, we conducted additional simulations without allowing evaporation. Those simulations resulted in multiple plausible reaction models for rainwater to C. Wink (table 4) but no plausible models for rainwater to PM-44, which suggests that diffusive, interplaya recharge (when it occurs) is accompanied by evaporation.

Accounting for intermediate mass transfers, such as those associated with surficial and vadose-zone C cycling, is problematic in inverse reaction-path modeling. Both rainwater and ground water are at or near equilibrium with atmospheric O_2 and contain little DOC, and only $\delta^{13}C$ and elevated HCO_3^- concentrations tend to preserve in ground water the evidence of OC oxidation during recharge. Moreover, it is uncertain whether oxidizing OC is primarily particulate (with resultant dissolution of CO_2 gas by recharging waters) (Wood and Petraitis, 1984) or dissolved. Forcing dissolution of CO_2 gas without including redox as a constraint or O_2 gas or CH_2O as phases resulted in multiple plausible reaction models for playa-focused recharge (with evaporation factors of 8.09 to 16.8) and one plausible model for interplaya recharge (with an evaporation factor of 8.51) (table 4). Discounting evaporation once again resulted in multiple plausible models for playa-focused recharge but no plausible models for interplaya recharge. While this approach is clearly a simplification of processes beneath playas, it may be more realistic in interplaya areas, in which a larger proportion of CO_2 is likely to be derived from root respiration (Bennett and others, 1995).

12

^{3}H concentrations indicate post-1952 recharge in the C. Wink well (1.84 TU) and possibly in PM-44 (1.2 TU in May 1994 [Argonne National Laboratory, 1994]). ^{14}C activities calculated by NETPATH for recharge to those wells depend upon the ^{14}C values specified for OC, CO_2 (g), and pedogenic soil carbonate (as $CaCO_3$). Although data are lacking for ^{14}C of $CaCO_3$, apparent ground-water ages $\leq$ ~40 yr (taken as the difference between calculated and observed ^{14}C activities) can be obtained using reasonable values for ^{14}C of CO_2 (g) (from table 1 of Thorstenson and others, 1983) and ^{14}C of OC. However, ^{14}C dating of recharge is problematic in part because of (1) the likelihood of mixing of ground waters of different ages (as noted previously) and (2) the likelihood that the ^{14}C activity of soil water is buffered by soil gas under open-system conditions (Plummer and others, 1994). Ingassing occurs when $^{14}CO_2$ concentrations in soil gas (which depend upon both the activity of ^{14}C and the mole fraction of CO_2) are greater than in soil water. Apparent ^{14}C ages of soil water from southern Nevada, where recharge has been negligible for thousands of years, were much younger than those determined by Cl^- mass balance calculations, which suggests diffusion and ingassing of $^{14}CO_2$ at depths of 30–146 m (Chapman and others, 1994; Tyler and others, 1995). In contrast, the rate of soil-water advection beneath playas is likely to be greater than that of gaseous diffusion, which raises the possibility of soil water dissolving $^{14}CO_2$ in the shallow subsurface and outgassing $^{14}CO_2$ deeper in the vadose zone. Without data on ^{14}C in soil water beneath playas, we cannot evaluate this possibility at present.

Potentiometric-surface mapping and ground-water flow modeling indicate that radial flow occurs within the perched aquifers. We modeled chemical evolution along a hypothetical transect from C. Wink to PM-44, ignoring interplaya recharge. However, no modeled combination of reactions could reproduce observed δ^{13}C (DIC) values in PM-44 within 4‰. Although the model parameters were not given, Argonne National Laboratory (1994, p. 4–33) also reported that "no reasonable model of chemical reactions in the (perched) aquifer results in the isotopic and chemical evolution of the low carbon isotope compositions to high carbon isotope compositions observed at Pantex." Ground-water compositions in PM-44, PM-101, PTX10-1007, and PTX10-1008 appear to reflect interplaya recharge of uncertain age. Lateral chemical evolution may occur naturally

within the perched aquifers closer to playas, but it appears to be masked by return flow in monitoring wells and in the E. Pratt well.

Perched Aquifers to Ogallala Aquifer

Reaction models were identified for pairs of Ogallala-aquifer wells located approximately along predevelopment ground-water flowlines. Between each pair of Ogallala-aquifer wells, we simulated mixing with water from the perched aquifers (C. Wink and/or PM-44) with and without reactions. These simulations necessitated the assumption, which will be addressed in more detail subsequently, that compositional evolution in the vadose zone between the perched aquifers and the Ogallala aquifer is negligible and that reactions occur in the Ogallala aquifer after mixing (if at all). We chose the same phases and constraints involved in modeling evolution of rainwater to perched ground water, except that we (1) excluded CH_2O as a phase, (2) specified no dissolution of calcite or CO_2 (g), and (3) used Cl^- and $\delta^{18}O$ to constrain mixing without reactions.

Because the perched aquifers are laterally extensive, and presumably separate water in the underlying vadose zone from $^{14}CO_2$ (g) in the overlying vadose zone, we assumed that ^{14}C could be used to calculate travel times between the perched and Ogallala aquifers ($t_{pc.-Og.}$) according to the equation:

$$t_{pc.-Og.} = (t_{mixed} - (t_{Og.-Og.} \times x_{Og.})) \times (x_{pc.})^{-1}.$$

Here, t_{mixed} is the ^{14}C "age" of the mixed water calculated by NETPATH, $t_{Og.-Og.}$ is the travel time between wells in the Ogallala aquifer, and $x_{pc.}$ and $x_{Og.}$ are the fractions of perched and upgradient Ogallala-aquifer water in the mixture, respectively. We determined ranges of $t_{Og.-Og.}$ from the predevelopment, steady-state potentiometric surface simulated by Mullican and others (1994), assuming an effective porosity (n_e) of 0.15 to 0.35 (Castany [1967], cited in de Marsily [1986, his fig. 2.17]). Using output files from the flow model MODFLOW (McDonald and Harbaugh, 1988) as input to MODPATH (Pollock, 1989), we generated forward and reverse particle tracks (at 10-yr time steps) from Ogallala-aquifer wells of interest. Forward tracks from

14

upgradient wells along transects were usually not identical to reverse tracks from downgradient wells; therefore, we visually estimated travel time along each particle track to a point parallel with the well of interest. Resulting values of $t_{Og.-Og.}$ ranged from 36 to 770 yr (table 5a).

Most models for which $\delta^{13}C$ was within 1‰ of observed and $t_{pc.-Og.}$ was >0, including all models allowing mixing without reactions, were still eliminated because $t_{pc.-Og.}$ exceeded $t_{Og.-Og.}$ by more than an order of magnitude. Travel times between playas and the perched aquifers (over distances greater than those separating the perched and Ogallala aquifers), as well as travel times across the perching strata calculated from Darcy's law (Mullican, 1995), are comparable to $t_{Og.-Og.}$. Moreover, given the hydrochemical and lithologic similarities between the perched and Ogallala aquifers, it is unlikely that reactions would occur during relatively short residence times in the Ogallala aquifer without having occurred (prior to mixing) during relatively long residence times in the overlying vadose zone. Plausible reaction models occur along a set of transects beneath Playa 1, from OM-105 to OM-39 and -40 and from OM-40 to PR-41 (table 5b; fig. 4). These models support petrographic observations of clay-mineral precipitation within the Ogallala aquifer. Percentages of perched ground water mixing with Ogallala-aquifer water along each transect ranged from 8.30 percent between OM-40 and PR-41 to 67.6 percent between OM-105 and OM-39. Plausible (positive) values of $t_{pc.-Og.}$ ranged from 19 yr between OM-105 and OM-39 ($n_e = 0.15$) to 2,400 yr between OM-40 and PR-41 ($n_e = 0.35$). Reaction models that mixed waters from both C. Wink and PM-44 with Ogallala-aquifer water yielded values of $t_{pc.-Og.}$ proportional to the amounts of water contributed from each of those wells. Not surprisingly, values of $x_{pc.}$ and $t_{pc.-Og.}$ appear to decrease and increase, respectively, with the depth of the screened interval in the Ogallala aquifer (compare OM-39 and OM-40 [table 5a]).

The selection of plausible reaction models should be viewed with caution because of various simplifications, some of which (for example, the selection of C. Wink and PM-44 to represent the compositions of perched ground water and the assumption of end-member aluminosilicate mineralogies) have already been noted. The assumption that chemical evolution in the lower vadose zone is negligible could be examined by forward reaction-path modeling using PHREEQE

Table 5(a). Approximate travel times, determined from particle tracks generated using MODPATH, between Ogallala-aquifer wells.

Upgrad. Og. well	Downgrad. Og. well	tOg.-Og. (yr) (n eff. = 0.15)	tOg.-Og. (yr) (n eff. = 0.25)	tOg.-Og. (yr) (n eff. = 0.35)
S. McGregor	OM-105	770	460	330
OM-105	OM-40	320	190	140
OM-105	OM-39	370	220	160
OM-105	OM-46	730	440	314
OM-105	OM-47	700	420	300
OM-105	OM-48	680	410	290
OM-40	PR-6	300	180	130
OM-40	PR-41	530	320	230
OM-39	PR-6	150	90	64
OM-39	PR-41	420	250	180
PR-6	PR-41	200	120	86
PR-41	PR-18	83	50	36

Table 5(b). Estimated ranges of travel times between the perched and Ogallala aquifers and fractions of water derived from the perched aquifer in downgradient Ogallala-aquifer wells, determined using NETPATH.

Upgrad. Og. well	Downgrad. Og. well	Perched well(s)	tpc.-Og. (yr) (n eff. = 0.15)	tpc.-Og. (yr) (n eff. = 0.25)	tpc.-Og. (yr) (n eff. = 0.35)	C. Wink wtr. (%)	PM-44 wtr. (%)	Total pc. wtr. (%)	Screen elev., downgrad. Og. well (m above sea level)
OM-105	OM-40	C. Wink+PM-44	730	1800	2200	3.04	7.65	10.7	888.2–897.3
OM-105	OM-39	C. Wink+PM-44	19	290	400	2.89	64.7	67.6	921.1-927.8
OM-105	OM-39	C. Wink+PM-44	1300	1600	1600	4.88	59.8	64.7	921.1-927.8
OM-40	PR-41	C. Wink	(-1000)	1300	2400	8.30		8.30	849.5–914.7
OM-40	PR-41	C. Wink+PM-44	(-2000)	(-570)	33	4.43	8.65	13.1	849.5–914.7
OM-40	PR-41	C. Wink+PM-44	(-2000)	(-560)	49	4.44	8.67	13.1	849.5–914.7
OM-40	PR-41	C. Wink+PM-44	(-880)	380	930	4.94	9.43	14.4	849.5–914.7

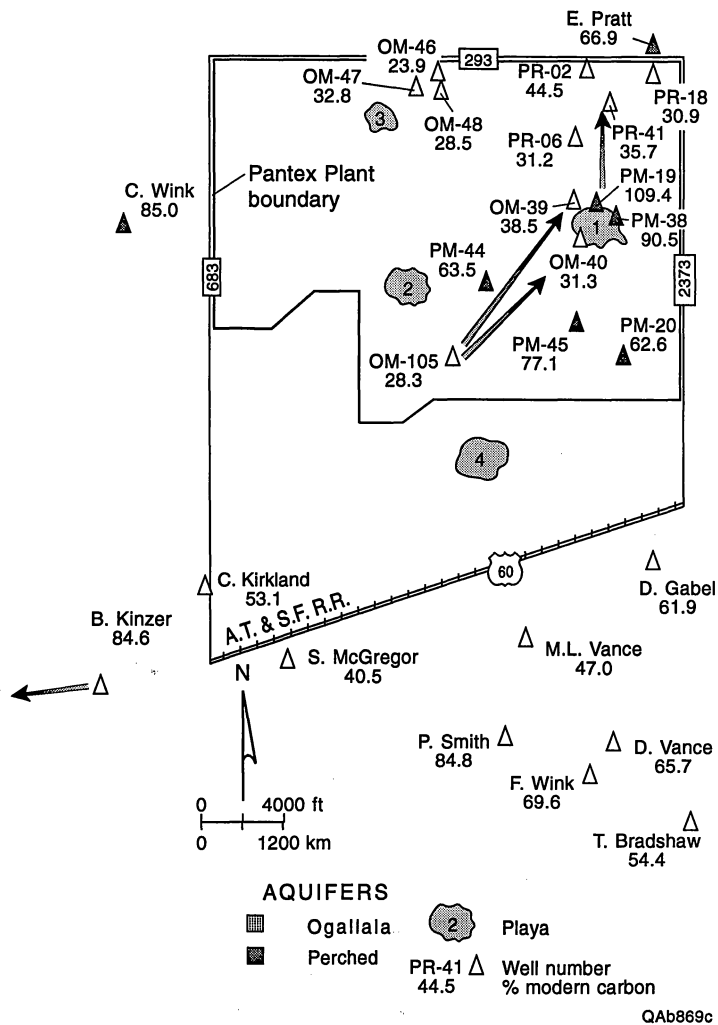Calculated values (in columns) that are less than zero are shown in parentheses.

16

Figure 4. Carbon-14 (^{14}C) abundances in the perched and Ogallala aquifers. Arrows show Ogallala-aquifer flow paths for which plausible-reaction path models were obtained.

17

(Parkhurst and others, 1980), but the assumption that ^{14}C in soil water is not buffered by $^{14}CO_2$ (g) can probably only be assessed by sampling in the lower vadose zone. We have assumed that despite extensive drawdown within the Ogallala aquifer, ground-water compositions are at steady state in wells unimpacted by return flow. In the absence of longer term monitoring, the lack of compositional trends in onsite Ogallala aquifer wells since 1991 (Battelle Pantex, 1992, 1993, 1994, 1995) supports this assumption. We have also assumed, as shown by Phillips and others (1989) for the Ojo Alamo and Nacimiento aquifers of the San Juan Basin, that hydrodynamic dispersion exerts a negligible influence on ^{14}C distributions. Our study is typical of regional-aquifer studies (for example, Plummer and others, 1990) in relying upon water-supply wells, which are commonly screened over thicknesses of meters to tens of meters. Sampling from such wells results in depth-integrated data masking vertical geochemical gradients (Ronen and others, 1987).

CONCLUSIONS

Chemical, isotopic, and mineralogical analyses indicate that the composition of ground water in the vicinity of the Pantex Plant reflects distinctive sources of recharge (both natural and anthropogenic) modified by sediment-water interactions, microbial processes, and some evaporation. Reaction-path modeling supports this conclusion and helps to constrain both percentages of perched ground water mixing with water in the Ogallala aquifer and travel times between the perched and Ogallala aquifers. Delineating sources of recharge and reactions is facilitated by the proximity of the study area to a hydrologic divide in the Ogallala aquifer, the presence of numerous wells in both the perched and Ogallala aquifers, and the existence of data from previous and concurrent regional investigations.

REFERENCES

Appelo, C. A. J., and Postma, D., 1993, Geochemistry, groundwater and pollution: Brookfield, Vermont, A. A. Balkema, 536 p.

Argonne National Laboratory, 1994, Draft phase I report and phase II work plan: expedited site characterization for the DOE Pantex Zone 12 groundwater investigation: prepared for U.S. Department of Energy, variously paginated.

Battelle Pantex, 1992, Pantex Plant environmental monitoring 1991 data compilation: prepared for the U.S. Department of Energy under DOE Grant No. DE-AC04-91AL65030, variously paginated.

Battelle Pantex, 1993, Pantex Plant environmental monitoring 1992 data compilation: prepared for the U.S. Department of Energy under DOE Grant No. DE-AC04-91AL65030, variously paginated.

Battelle Pantex, 1994, Pantex Plant environmental monitoring 1993 data compilation: prepared for the U.S. Department of Energy under DOE Grant No. DE-AC04-91AL65030, variously paginated.

Battelle Pantex, 1995, Pantex Plant environmental monitoring 1994 data compilation: prepared for the U.S. Department of Energy under DOE Grant No. DE-AC04-91AL65030, variously paginated.

Bennett, P. C., Hua, H.-P., Kirschenmann, K., Minehardt, T. J., Nicot, J.-P., and Romanak, K. D., 1995, Geochemical controls on organic contaminants in the vadose zone, *in* Gustavson, T. C., and others, Summary hydrogeologic assessment, U.S. Department of Energy Pantex Plant, Carson County, Texas: report prepared for the U.S. Department of Energy under subgrant to DOE Grant No. DE-FG04-90AL65847, p. 87–98.

Blair, N., Leu, A., Munoz, E., Olsen, J., Kwong, E., and des Marais, D., 1985, Carbon isotopic fractionation in heterotrophic microbial metabolism: Applied and Environmental Microbiology, v. 50, p. 996–1001.

Bruggenwert, M. G. M., and Kamphorst, A., 1982, Survey of experimental information on cation exchange in soil systems, *in* Bolt, G. H., ed., Soil chemistry, B. Physico-chemical models: New York, Elsevier, p. 141–203.

Castany, G., 1967, Traité pratique des eaux souterraines, 2d ed.: Paris, Dunod.

Chapman, J. B., Tyler, S. W., Davisson, M. L., and Shadel, C. A., 1994, Carbon-14 age dating of soil water from a thick vadose zone in southern Nevada (abs.): Geological Society of America Abstracts with Programs, v. 26, no. 7, p. A-390.

de Marsily, G., 1986, Quantitative hydrogeology, groundwater hydrology for engineers: Orlando, Academic Press, 440 p.

Dugan, J. T., McGrath, T., and Zelt, R. B., 1994, Water-level changes in the High Plains aquifer—predevelopment to 1992: U.S. Geological Survey Water-Resources Investigations Report 94-4027, 56 p.

Eslinger, E., and Pevear, D., 1988, Clay minerals for petroleum geologists and engineers: Society of Economic Paleontologists and Mineralogists Short Course Notes No. 22, variously paginated.

Freeze, R. A., and Cherry, J. A., 1979, Groundwater: Englewood Cliffs, New Jersey, Prentice-Hall, 604 p.

Hendry, M. J., and Schwartz, F. W., 1990, The chemical evolution of ground water in the Milk River aquifer, Canada: Ground Water, v. 28, no. 2, p. 253–261.

Keeling, C. D., 1958, The concentration and isotopic abundance of atmospheric carbon dioxide in rural areas: Geochimica et Cosmochimica Acta, v. 13, p. 322–334.

Keller, C. K., 1991, Hydrogeochemistry of a clayey till, 2. Sources of CO_2: Water Resources Research, v. 27, no. 10, p. 2555–2564.

Knowles, T. R., Nordstrom, P., and Klemt, W. B., 1982, Evaluating the ground-water resources of the High Plains of Texas, final report, basic data for the northern third of region: Texas Department of Water Resources Report LP-173, v. 2, 451 p.

McDonald, M. G., and Harbaugh, A. W., 1988, A modular three-dimensional finite-difference ground-water flow model: U.S. Geological Survey Techniques of Water-Resources Investigations, bk. 6, variously paginated.

Mook, W. G., 1980, Carbon-14 in hydrogeological studies, *in* Fritz, P., and Fontes, J.-C., eds., Handbook of environmental isotope geochemistry, volume 1, the terrestrial environment, A, ch. 2: New York, Elsevier, p. 49–74.

Mullican, W. F., III, 1995, Saturated-zone hydrology, *in* Gustavson, T. C., and others, Summary hydrogeologic assessment, U.S. Department of Energy Pantex Plant, Carson County, Texas: report prepared for the U.S. Department of Energy under subgrant to DOE Grant No. DE-FG04-90AL65847, p. 59–75.

Mullican, W. F., III, Johns, N. D., and Fryar, A. E., 1994, Calibration and sensitivity analysis of an Ogallala aquifer ground-water flow model: The University of Texas at Austin, Bureau of Economic Geology, milestone report prepared for the U.S. Department of Energy under subgrant to DOE Grant No. DE-FG04-90AL65847, 82 p.

Murphy, E. M., Schramke, J. A., Fredrickson, J. K., Bledsoe, H. W., Francis, A. J., Sklarew, D. S., and Linehan, J. C., 1992, The influence of microbial activity and sedimentary organic

carbon on the isotope geochemistry of the Middendorf aquifer: Water Resources Research, v. 28, no. 3, p. 723–740.

Nativ, R., 1988, Hydrogeology and hydrochemistry of the Ogallala aquifer, Southern High Plains, Texas Panhandle and New Mexico: The University of Texas at Austin, Bureau of Economic Geology Report of Investigations No. 177, 64 p.

Parkhurst, D. L., Thorstenson, D. C., and Plummer, L. N., 1980, PHREEQE—A computer program for geochemical calculations: U.S. Geological Survey Water-Resources Investigations Report 80-96, 210 p.

Phillips, F. M., Tansey, M. K., Peeters, L. A., Cheng, S., and Long, A., 1989, An isotopic investigation of groundwater in the central San Juan Basin, New Mexico: carbon 14 dating as a basis for numerical flow modeling: Water Resources Research, v. 25, no. 10, p. 2259–2273.

Plummer, L. N., Busby, J. F., Lee, R. W., and Hanshaw, B. B., 1990, Geochemical modeling of the Madison aquifer in parts of Montana, Wyoming, and South Dakota: Water Resources Research, v. 26, no. 9, p. 1981–2014.

Plummer, L. N., Prestemon, E. C., and Parkhurst, D. L., 1994, An interactive code (NETPATH) for modeling net geochemical reactions along a flow path, version 2.0: U.S. Geological Survey Water-Resources Investigations Report 94-4169, 130 p.

Pollock, D. W., 1989, Documentation of computer programs to compute and display pathlines using results from the U.S. Geological Survey modular three-dimensional finite-difference ground-water flow model: Washington, D.C., Scientific Software Group, variously paginated.

Robie, R. A., Hemingway, B. S., and Fisher, J. R., 1978, Thermodynamic properties of minerals and related substances at 298.15K and 1 bar (10^5 pascals) pressure and at higher temperatures: U.S. Geological Survey Bulletin 1452, 456 p.

Ronen, D., Magaritz, M., Almon, E., and Amiel, A. J., 1987, Anthropogenic anoxification ("eutrophication") of the water table region of a deep phreatic aquifer: Water Resources Research, v. 23, no. 8, p. 1554–1560.

Steefel, C. I., and van Cappellen, P., 1990, A new kinetic approach to modeling water-rock interaction: The role of nucleation, precursors, and Ostwald ripening: Geochimica et Cosmochimica Acta, v. 54, p. 2657–2677.

Suchomel, K. H., Kreamer, D. K., and Long, A., 1990, Production and transport of carbon dioxide in a contaminated vadose zone: a stable and radioactive carbon isotope study: Environmental Science and Technology, v. 24, p. 1824–1831.

Tardy, Y., 1971, Characterization of the principal weathering types by the geochemistry of waters from some European and African crystalline massifs: Chemical Geology, v. 7, p. 253–271.

Thorstenson, D. C., Weeks, E. P., Haas, H., and Fisher, D. W., 1983, Distribution of gaseous $^{12}CO_2$, $^{13}CO_2$, and $^{14}CO_2$ in the subsoil unsaturated zone of the western Great Plains of the U.S.: Radiocarbon, v. 25, p. 315–346.

Tyler, S. W., Chapman, J. B., Conrad, S. H., and Hammermeister, D., 1995, Paleoclimatic response of a deep vadose zone in southern Nevada, U.S.A., as inferred from soil water tracers, *in* Proceedings, First International Symposium on Tracers in Arid Zones: Vienna, International Atomic Energy Agency, in press.

Wood, W. W., and Petraitis, M. J., 1984, Origin and distribution of carbon dioxide in the
unsaturated zone of the Southern High Plains of Texas: Water Resources Research, v. 20,
no. 9, p. 1193–1208.

Zwingle, E., 1993, Ogallala aquifer, wellspring of the High Plains: National Geographic, v. 183,
no. 3, p. 80–109.